PRAMANA
— journal of
physics

Vol. 85, No. 2
August 2015
pp. 267–280

Statistical and dynamical aspects in fission process: The rotational degrees of freedom

BENCY JOHN
Nuclear Physics Division, Bhabha Atomic Research Centre, Mumbai 400 085, India
E-mail: bjohn@barc.gov.in, bencyv.john@gmail.com

DOI: 10.1007/s12043-015-1041-5; ***e*Publication:** 29 July 2015

Abstract. In the final phases of fission process, there are fast collective rotational degrees of freedom, which can exert a force on the slower tilting rotational degree. Experimental observations that lead to this realization and theoretical studies that account for dynamics of the processes are discussed briefly. Supported by these studies, and by assuming a conditional equilibrium of the collective rotational modes at a pre-scission point, a new statistical model for fission fragment angular and spin distributions has been developed. This model gives a consistent description of the fragment angular and spin distributions for a wide variety of heavy- and light-ion-induced fission reactions.

Keywords. Fission process; nucleon exchange; collective rotational modes; conditional equilibrium; fragment angular distributions; fragment spins.

PACS Nos 24.10.−I; 25.70.Jj; 25.85.Ge

1. Introduction

It is of basic interest to understand the interplay of statistical and dynamical aspects in the fission process, during the evolution from compound nucleus to the formation of pre-fragments and their final emission. In the multidimensional potential energy surface, the fission proceeds in the 'fission valley' direction, and encounters quasiequilibrium and out-of-equilibrium events and phases, extreme deformations, and dinuclear configurations en route. Several additional nuclear collective and intrinsic degrees of freedom emerge and several disappear during the course of this journey. A 'shape-dynamics' approach was adopted in several fission studies in the past to understand these emergences and dissolutions but with a limited success [1,2]. It was observed that the internal structure of the nucleus influences the dynamics of collective motion towards fission. Two extreme assumptions can be made about the coupling between the collective and internal degrees namely, weak and strong. The two assumptions gave rise to two principal branches of the liquid drop-based models: adiabatic and statistical. A purely statistical

description calculates the phase-space using the energy available above the nuclear potential energy surface, and the impacts of the saddle or the scission configurations are estimated from the phase-space arguments. In a more evolutionary dynamical approach, which is a refined version of the adiabatic model, at each deformation step, the impacts of its previous step and the impacts on the following one are estimated till one gets to the final split. The generation of collective kinetic energy and transfer of energy between the internal and collective degrees of freedom are integrated to this approach. It may be noted that the statistical models often provide good insights into the nuclear behaviour which the complete (never so far realized) dynamical theory ought to predict, and a remarkable phenomenological power within their own range of relevance.

Models of statistical equilibrium near the scission point have been used for many aspects of particle-induced fission such as mass distribution, TKE distribution, fragment spin, excitation energy distribution, etc. However, for the fragment angular distributions, there have been some reservations in using the scission point model. One of the reasons could be that the formulas derived under certain 'reasonable' assumptions yielded substantially higher values of anisotropy when compared with the experimental data. As it is shown in the following sections, the alternate statistical models for angular distribution based on the equilibration at saddle point are also riddled with several problems in interpreting the data on many related aspects in fission. A conditional equilibrium of collective and internal degrees of freedom in statistical description with the pre-scission stage as the transition state can solve this impasse as shown in [3] and this approach is discussed in §4 in some detail. Angular momentum bearing collective modes have a major role in this model and in the following section a brief introduction to these modes is given.

2. Rotational degrees of freedom in fissioning nuclei

In heavy-ion fusion process, the couplings of the relative motion to collective and internal degrees of freedom lead to the transfer of orbital angular momentum to nuclear spin – from pure orbital motion to all the way down to rigid rotation. In the fissioning nucleus, a reverse do also happen; as the nucleus elongates and pre-fragments are formed, the total angular momentum J (initially in rigid rotation) can partition gradually into an orbital component (R) and an intrinsic component (K). In addition to the rigid rotor degrees of freedom, other intrinsic angular momentum bearing modes are also active in the fission process. This became evident with the observation of sizable amount of angular momentum ($\sim 8\hbar$) in fission fragments from the spontaneous fission of ^{252}Cf where the nucleus is initially in $J = 0$ state. Since then, several studies have been carried out, and in recent years, by using high efficiency gamma spectrometry tools and extensive database-supported analysis techniques, access to angular momentum distribution in fragments produced in thermal neutron and spontaneous fissions has improved considerably [4]. Similar works have been extended to higher excitation energies and also in heavy-ion-induced fission reactions. It has been observed that a rather high angular momentum population in fission fragments is a general property of all types of fission processes.

The origin of this sizable angular momentum, which is aligned roughly perpendicular to the fission axis, well beyond what the rigid rotational modes can impart, remains an intriguing aspect of the fission process. Several theoretical studies have been conducted

on this aspect and most of them depend rather sensitively on the deformation of the fragments at a final scission (dinuclear) configuration. The balance of repulsive Coulomb and attractive nuclear forces between the tips of the fragments facing each other is an essential aspect to induce bending, twisting, and wriggling modes of vibrations, either by zero-point oscillations or in the case of a finite temperature at the scission, by thermal excitations [5,6]. Situations in which the balance of forces are such that the fragments from tip to tip are completely aligned along the axis are considered in a quantum mechanical approach. This resulted in a new orientation pumping mechanism for generation of fragment angular momentum as discussed in detail in [7]. These theories rely almost exclusively on the dinuclear scission configuration to operate the spin generation mechanism. This is in some way analogous to nuclear molecular resonances in light nuclei where one considers the relative motion of the two nuclei [8]. The theoretical models are rather silent on angular momentum modes that impart spin to pre-fragments before the final scission stage.

A more justifiable but a complex way to consider generation of angular momentum bearing collective rotational currents would begin at an earlier stage than at the final scission stage. Elongation and necking-in occur in a fissioning nucleus at gradually increasing levels right from the onset and this process is initiated by net transfer of nucleons to two opposite directions within the nucleus. When necking-in picks up at later stages, the nucleons remaining in the midregion are swept towards left and right to the forming pre-fragments. This net transfer of nucleons causes a mononucleus to become a dinucleus, and the transition stage, where the nucleus behaves as both mononucleus and dinucleus simultaneously, can be termed as the pre-scission configuration [3].

From extensive studies of dinuclei formed in damped nuclear collisions, a phenomenon that has many parallels to the fission process though it is a much faster process, such net nucleon transfers are understood as due to a mechanism where individual nucleons are exchanged between the reaction partners [9–11]. Macroscopic degrees of freedom that are special to dinucleus identified are: (i) the energy associated with relative nuclear motion and (ii) the partition of microscopic excitation energy, total mass, charge and angular momenta among the two parts of the dinucleus. This formalism has also been extended to the more intimate and longer lasting quasifission reactions. The problem of accumulation of angular momentum in damped collisions and quasifission are addressed in [10,11]. In the above studies, the underlying mechanism of nucleon exchange between two nuclei is very similar to that employed earlier by Ramanna *et al* [12,13] to describe the fission process. In [12,13], the fragment mass and charge distributions in low energy fission were investigated in detail with realistic inputs for the nucleon transfer probabilities. However, angular momentum generation has not been explicitly treated.

It is instructive to enumerate the translational and rotational degrees of freedom of a dinuclear system before considering the same in a pre-scission shape. The dinucleus, if considered as two rigid bodies, require $6 + 6 = 12$ degrees of freedom. The condition of contact removes one. From the remaining, three are translational degrees of freedom, so there are totally eight rotational degrees of freedom [14,15]. Of these eight, three are associated with rigid rotations (mentioned in the beginning of this section) of the dinuclear system. The remaining five are intrinsic angular momentum-bearing modes, which are rotations of one nucleus with respect to other in such a way that the whole system has no net angular momentum. These are two degenerate bending modes, two degenerate

wriggling modes, and one twisting mode. A reference to angular momentum degrees of freedom at a pre-scission stage is made by Nix and Swaitecki [16], where a nucleus prior to division was represented by two overlapping spheriods, with the interior surface of each simply erased. The sequence of shapes of a fissioning nucleus from the original sphere to two fragments at infinity are approximately described. The two-spheroid model has been useful for estimating the distributions in mass, total translational kinetic energy, and fragment excitation energies. Classical dynamical equations of motion were used for solving the motion of the system from the given initial configuration near the saddle point to the final configuration of the two fragments at infinity. The use of classical equations of motion for the separation of fragments to infinity may be partially justified on the grounds that at a short distance from the saddle point, the de Broglie wavelength for translational motion is relatively small, and the rotations or vibrations about each fragment's centre-of-mass involve several quanta of energy and angular momentum.

Various angular momentum-bearing collective modes and their relaxation times in a pre-scission nucleus are briefly reviewed in [3]. The pre-scission configuration is just a tracing back of the dinuclear scission stage into the internals prior to scission and contains the physics shortly before the final split. Figures 1a–1c schematically depict the rotational motion in a pre-scission nucleus using arrows. The criteria for selecting this pre-scission shape are discussed in §4. In this picture, the nucleons have been considered as classical particles fully localizable in phase-space. The volume from which the nucleons finally recede to prefragments due to progressive elongation and necking, is spatially confined (on the average) to the middle region. Let us first consider the wriggling and twisting modes that are excited by fast elementary nucleon transfer processes in the symmetric division of nucleus. These modes, while conserving the total angular momentum, impart angular momenta to the prefragments. The thick curved arrows in figure 1b indicate the

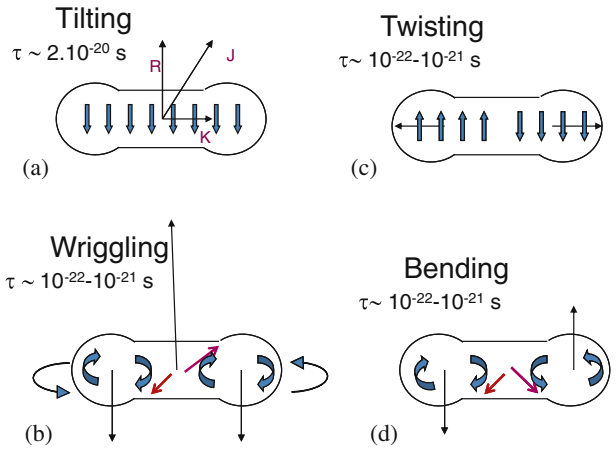

Figure 1. A schematic illustrating the collective angular momentum-bearing modes in a pre-scission nucleus. The thick arrows indicate the velocity fields associated with these modes. The thin straight arrows indicate the directions of the imparted spins. In (**a**), the vectors J, R, and K show the total angular momentum, orbital angular momentum, and the tilting angular momentum, respectively, of the fissioning nucleus (from [3]).

velocity fields associated with the wriggling motion. The counter-rotation is also indicated. The thin straight arrows indicate the direction of spins thus imparted in the prefragments. The fast elementary nucleon transfers that strongly excite the wriggling mode are the long mean free path nucleon movements in opposite directions. These transfers cause a net mass drift from the central region to the forming prefragments. The pair of short arrows in figure 1b schematically show two such nucleon transfers. Although it is not necessary that these nucleon transfers occur simultaneously and they are of exactly opposite momentum magnitudes, these qualities are to be maintained on the average, over a suitable short time period. If they are not maintained, then one would have to admit a momentum imbalanced nucleon flow to one of the prefragments. Additionally, these basic microscopic processes in the system are to be consistent with the one-body dissipative mechanisms for energy and angular momentum dissipation. The same arguments can be extended to asymmetric mass division as well, where a larger number of transferred nucleons to the heavy fragment side can be compensated by higher velocity transfers of lower number of nucleons to light fragment side. Similar nucleon transfer mechanism causes twisting mode of rotation where fragment spins are along the axis but in opposite directions (figure 1c). The bending mode requires nucleon transfers such as represented by a pair of short arrows in figure 1d if they are to be excited. However, such microscopic processes are unlikely [3] because they create momentum imbalances and spurious motions of the centre of mass. The nucleon transfers cannot directly excite the tilting mode K but it is excited indirectly through the (Coriolis) coupling induced by the orbital rotation [10].

Quantitative estimates of relaxation times of rotational modes discussed above are not available. Nevertheless, the estimates reported for nucleus–nucleus collisions where these modes are excited can be used as guidelines. In [10], the dynamical evolution of a dinucleus formed in nucleus–nucleus collision is discussed in terms of the time-dependent relaxation times associated with the rotational modes. For the fission case, where scope for particle exchange between two forming partners is large till the final split, meaningful comparisons can be made with the local relaxation times calculated for the turning point of relative motion in the nucleus–nucleus collision. It has been shown [10] that for angular momentum values typical of heavy-ion-induced fission reactions, the relaxation time for the tilting mode is fairly long compared to the other modes. Typically, the relaxation time for the tilting mode is around 2×10^{-20} s whereas for the fast modes it is around 3×10^{-22} s.

3. Experimental observations

3.1 *Fragment angular distributions in particle-induced binary fission*

For an axially-symmetric fissioning nucleus of total angular momentum J, its projection on a space-fixed axis M, and its projection on the nuclear symmetry axis K, the final fragment angular distribution can be described using properly weighted rotational wave function $D^J_{MK}(\theta)$, where θ is measured with respect to the space-fixed axis, provided one knows weighting functions for final values of J, M, and K. As J and M are conserved throughout the process, knowledge of their initial populations would define their weighting functions. In case of K, which is not conserved in the fission process because the

orientation of the symmetry axis can change by thermal agitations, certain assumptions are made regarding its approximate conservation and final population distribution. It is assumed that a final stage of quasiequilibrium for K can be identified and, while evolving ahead from this stage, the K is frozen and hence it remains as a good quantum number till the fragments are finally emitted. This stage is called the transition state and the model for angular distributions based on this idea is called the statistical transition state model (TSM).

There has been a great deal of discussion on whether to identify the transition state with the saddle or with the scission-point deformations [17–21]. In light-ion-induced fission of actinide nuclei, the experimental information on this critical deformation tilted the balance towards the saddle-point model [21]. In heavy-ion-induced fission, where high angular momentum and excitation energy states are populated, the experimental data did not allow a clear-cut conclusion regarding the question of saddle or scission-point models. For these systems of high angular momentum and Z^2/A values, the saddle-point model predicts small angular anisotropies because the relevant saddle-point shapes are nearly spherical. Statistical scission-point models [18,19] in which the critical deformation is the scission point, on the other hand, predict large angular anisotropies. Experimental values are spread in between these predictions [20]. The high angular anisotropies observed in systems which bear characteristics of fast decay processes such as asymmetric angular distributions and incompletely relaxed mass distributions were interpreted on the basis of fast fission or quasifission [22]. However, there are many instances where anisotropy values are in disagreement with both the saddle and scission-point model predictions, even though there are no clear signatures of fast decay processes. For instance, the experimentally determined values of $\mathcal{J}_0/\mathcal{J}_{\rm eff}$ from fission reactions induced by projectiles with mass less than or equal to 24 in the compound nuclear (CN) fissility range from 0.76 to 0.88 are compared with the expected saddle-point value of $\mathcal{J}_0/\mathcal{J}_{\rm eff}$ from RLDM [22] in figure 2, as ratio of the two, given by $\mathcal{J}_{\rm eff}^{\rm RLDM}/\mathcal{J}_{\rm eff}^{\rm EXPT}$. In this set of reactions there are very little chances of fast reactions and the selected ones populate fusion–fission reactions with saddle temperatures in the range 1.1–2.2 MeV. However, the ratio $\mathcal{J}_{\rm eff}^{\rm RLDM}/\mathcal{J}_{\rm eff}^{\rm EXPT}$, obtained by averaging over the above temperature range, showed considerable spread instead of converging to unity, as seen in figure 2. A recent reanalysis in a few of the above reactions [23], that took into account the effects of pre-scission neutron emissions, could not discard this anomaly and it is noted that the saddle-point TSM is inapplicable

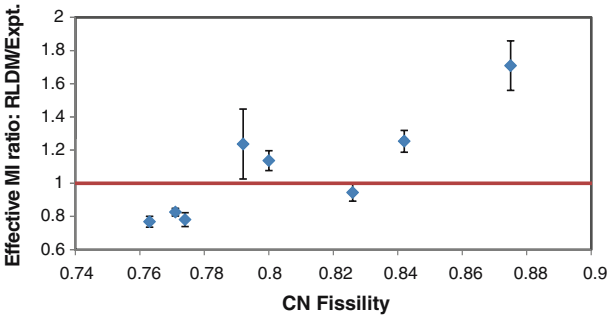

Figure 2. Effective moment of inertia ratio $\mathcal{J}_{\rm eff}^{\rm RLDM}/\mathcal{J}_{\rm eff}^{\rm EXPT}$ vs. compound nucleus fissility.

to very heavy compound nuclei such as ^{254}Fm and ^{264}Rf that have fission barrier heights comparable with the temperatures of the compound nuclei.

3.2 *Fragment mass and angular anisotropy correlation*

In equilibrium fission, a correlation between fragment angular and mass distributions beyond particle emission corrections can arise provided there are some meaningful differences in the distribution of rotational quantum numbers for different modes of mass division. For fission induced by light particles like n, p, and α, the total angular momenta J are generally low and the influence of K on this correlation has been examined [24,25]. For heavy-ion reactions, both J and K can influence this correlation [26]. A comprehensive analysis of the experimental data using theoretically generated correlations has not been done yet. For instance, for the ^{10}B+^{232}Th and ^{16}O+^{232}Th reactions studied in [26], the compound nuclear parameters are such that the standard saddle-point TSM predicts the same value of angular anisotropy for all masses (horizontal line in figure 3). However, the experimental data show significant deviations from this value with a certain clear pattern (symbols in figure 3), with differing magnitudes for the two reactions. Pre-saddle neutron emission or influences of transfer-induced fission or pre-equilibrium fission cannot explain this observation adequately [26].

3.3 *Gamma multiplicity*

Another experimental approach which probes the equilibration of the rotational degrees of freedom is to measure the average fragment angular momentum and its angular variation [27] using gamma multiplicity (M_γ) set-ups. As theoretical prediction of the average total fragment angular momentum and its angular variation involves some of the same parameters as the fragment angular distributions, one should be able to reproduce consistently, both the fragment angular anisotropy and spin data, in the same model calculation.

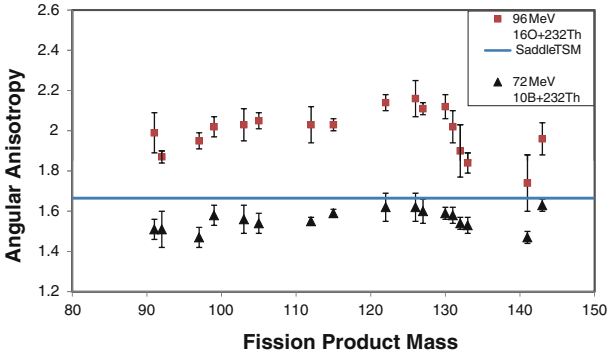

Figure 3. Experimental data on angular anisotropy vs. fission product mass measured using recoil catcher technique in the two reactions explained in §3.2. Experimental data are from [26]. The horizontal line is the value of anisotropy calculated using the saddle-point TSM which is very nearly the same for the two reactions [26].

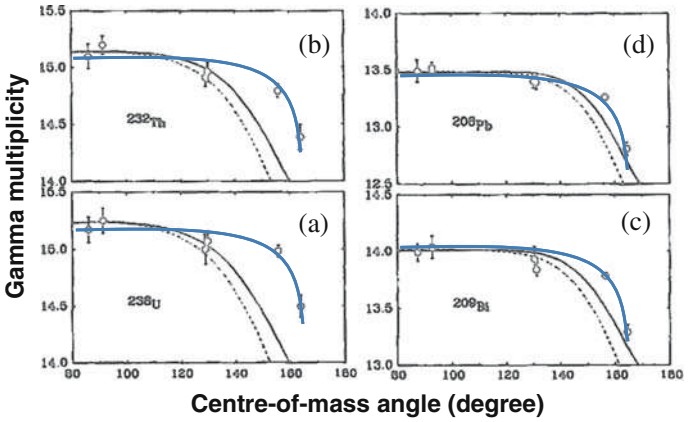

Figure 4. **(a)–(d)** Gamma multiplicity as a function of the centre-of-mass angle for several 120 MeV ^{16}O-induced fission reactions on targets as explained in §3.3. Experimental data are given by the symbols. The dotted and thin solid lines indicate scission-point and saddle-point TSM predictions, respectively. The thick solid curves are experimental trend lines which are identical curves except for the heights. Experimental data and model calculations are from [27].

Systematic investigations in both light- and heavy-ion-induced fissions have shown that the experimental data can only be explained by assuming substantial thermal excitation of the collective angular momentum-bearing modes, with the assumption of spin equilibrium at rather elongated configurations like the scission point [27]. Notable features of the angular variation of M_γ are that M_γ decreases rather very slowly with angle for a wide window of angles ($\pm 60°$) centred at 90° in c.m. system, and beyond this window, it decreases more rapidly. The overall variations does not show any systematic dependence on the fissility of the compound nuclei (figure 4). The experimental trends are in contrast to the predictions of the saddle and scission-point versions of the TSM.

3.4 *Angular anisotropy and total fragment spin: Empirical correlations*

Experimental investigations approached the question on how strong is angular anisotropy and total fragment spin correlation in two ways. In the first investigation by Ogihara *et al* [28], the systematics of the decoupling angle θ_0 was obtained by measuring the fragment angular distributions precisely in a number of heavy-ion-induced compound nuclear fission reactions. In a precise and accurate angular distribution, a strong smearing from $1/\sin(\theta)$ form factor arises due to the decoupling of orbital angular momentum R from total angular momentum J due to the presence of total fragment (exit channel) spin S. One must consider averaged quantities when comparing with the measured data, and the decoupling angle θ_0 is assumed to be related to the average angular momentum according to the model of Ericson [29], as $\sin(\theta_0) = \langle S\rangle/\langle J\rangle$, where $\langle S\rangle$ is the average exit channel spin and $\langle J\rangle$ is the average CN angular momentum. It is experimentally observed [28] that the anisotropy scales with the decoupling angle indicating a strong correlation between anisotropy and average exit channel spin $\langle S\rangle$. The second investigation [30], on the other hand, measured the average exit channel spin $\langle S\rangle$ through average gamma

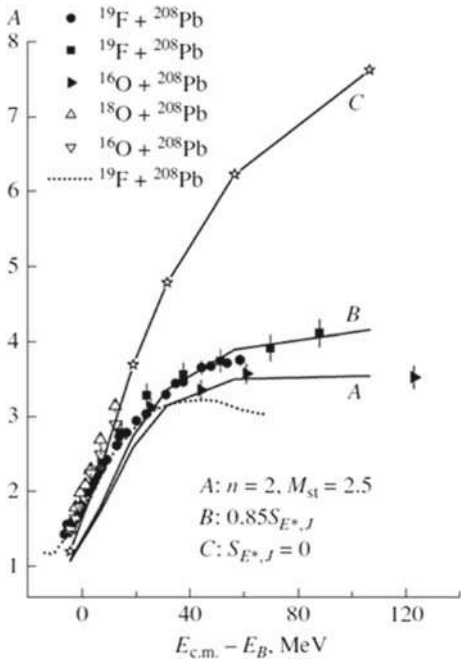

Figure 5. Fission fragment angular anisotropy A vs. 'energy above Coulomb barrier' $E_{\text{c.m.}} - E_{\text{B}}$ for the reactions as explained in §3.4 [30]. The dotted curve shows the results of saddle-point TSM calculation for the $^{19}\text{F}+^{208}\text{Pb}$ reaction [31]. See text for details on the calculations which resulted in Curves A, B and C.

multiplicity in a heavy-ion-induced fission reaction over a broad range of bombarding energies and found that it is strongly correlated to the observed angular anisotropy in the reaction (under certain assumptions). The anisotropy data used in this analysis [22,31,32] are shown in figure 5 as a function of the 'energy above Coulomb barrier', $E_{\text{c.m.}} - E_{\text{B}}$. The dotted curve shows the results of saddle-point TSM calculation for anisotropy for the $^{19}\text{F}+^{208}\text{Pb}$ reaction [31]. Other curves in figure 5 have been obtained as follows: On the condition of complete alignment of the 'excited' angular momentum due to collective spin modes, the total value of which is empirically deduced, the angular anisotropy vs. $E_{\text{c.m.}} - E_{\text{B}}$ relation was calculated by assuming the scission-point TSM, as given by curve A. By allowing only a 0.85 factor for such an alignment, the results were recalculated as given by curve B. Scission-point prediction without alignment (factor $= 0$) is given by curve C. This empirical study shows that the scission-point TSM with a conditional equilibration for obtaining $\langle R^2 \rangle$ explains the data on fragment spins and angular anisotropies. However, the physical interpretation behind this conditional equilibration has not been made clear in these studies.

4. Statistical pre-scission point model of fission fragment angular distribution

As discussed in §3, a comprehensive re-examination of various experimental and statistical model results concerning the rotational degrees of freedom in equilibrium fission

aggravated the problems in understanding the fission process, particularly the final phases of fission. The collective rotational degrees associated with the final phase of fission seem to be influencing the fragment angular distributions. However, the absence of successful models which can describe this influence inhibited the progress in understanding the fission process. At the outset, the configurations at which the statistical model can be applied needs careful considerations as one is dealing with an overall out-of-equilibrium process. This problem involves not just one property of the system like its potential energy surface but also the formation dynamics of prefragments and their interactions. A two-stage description has been proposed in a microscopic study of nuclear scission and quantum localization in [33]. According to this work, from the onset as one approaches the scission point, the prefragments emerge into existence, and as a result, the values of the global constraints split into the contributions from these prefragments. It is expected that the correct description of the system will rely on separate collective coordinates for these individual prefragments. The statistical pre-scission point model imbibes this spirit in defining the pre-scission configuration. However in the present version, relatively simple shape parametrizations, that account for essentials of the random neck rupture model [34], have been used to predict the pre-scission shapes [3].

The novel idea in this model is the conditional equilibrium of angular momentum-bearing collective modes. As the wriggling and twisting modes relax rapidly compared to the tilting mode, one can calculate the population probability for these modes for a tilted pre-scission nucleus. It is shown that for the tilting angular momentum states ($|K|$) near zero, the wriggling and twisting mode populations are maximum and as $|K|$ increased, these populations decrease. As the energy locked in these collective modes are not available for intrinsic excitations, the phase-space available at the transition state gets modified accordingly. The method for calculating the phase-space factor is described in detail in [3]. As an example, the average rotational energies of thermally excited wriggling ($E^K_{\rm wri}$) and twisting ($E^K_{\rm twi}$) modes, for a pre-scission nucleus of mass $A = 225$ and temperature $T = 2$ MeV as a function of tilting mode angular momentum K are given in figure 6 as sums over the tilting mode energy $E^K_{\rm tilt}$. For K near zero, the wriggling and twisting mode contributions are large and as $|K|$ increased, this contribution decreased. The average wriggling rotational energy is significantly higher than the average twisting rotational energy. The total rotational energy as a function of J and K is obtained as

$$E^{J,K}_{\rm rot} = E^J_{\rm yrast} + E^K_{\rm tilt} + E^K_{\rm twi} + E^K_{\rm wri}. \tag{1}$$

The transition state level density $\rho(E^*, J, K)$ is obtained by assuming constancy of nuclear temperature T at the pre-scission state as

$$\rho(E^*, J, K) \propto \exp\left(\frac{E^* - E^{J,K}_{\rm rot}}{T}\right), \tag{2}$$

where $E^* = E_{\rm CN} - E_{\rm p} - E_{\rm def}$, $E_{\rm CN}$ is the initial excitation energy of the CN, $E_{\rm p}$ is the average excitation energy taken away by the particles emitted prior to the transition state, and $E_{\rm def}$ is the deformation energy of the transition state. The resulting $\rho(E^*, J, K)$, after expansion, will not have a Gaussian K distribution.

Using the above modified phase-space factor, the fragment angular distributions were calculated for a large set of reactions leading to compound nuclei in the fissility range of 0.76 to 0.88 and initial temperature range of 1 to 4 MeV, as given by continuous lines in

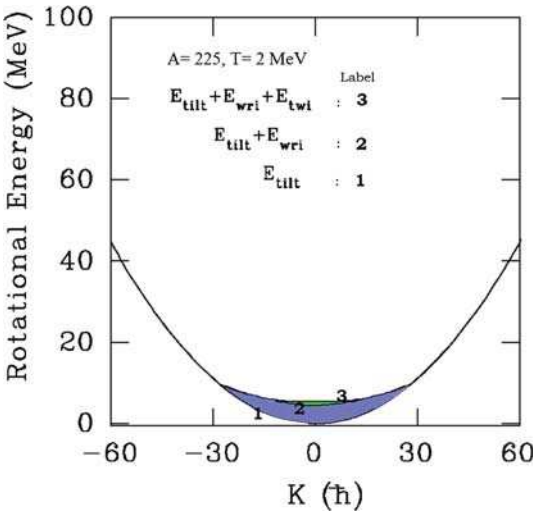

Figure 6. Average rotational energies of thermally excited wriggling ($E^K_{\rm wri}$) and twisting ($E^K_{\rm twi}$) modes for a pre-scission nucleus of mass $A = 225$ and temperature $T = 2$ MeV as a function of tilting mode angular momentum K, showing sums over the tilting mode energy $E^K_{\rm tilt}$ [3].

figures 7a–7j [3]. Experimental angular anisotropy data for these systems [22,35,36] are plotted in figure 7 using symbols. The set of common parameters and procedures used in the calculations are given in detail in [3]. In addition to the present statistical pre-scission model calculations, the results obtained using the scission-point models of Bond [18] and Rossner *et al* [19] are given in figures 7a–7j as short dashed and dashed lines. The long dashed lines indicate the results obtained using the pre-scission shape as transition configuration without the rotational energy corrections due to the wriggling and twisting modes. There is a remarkable improvement in the agreement between the experimental data and the pre-scission-point model calculations (continuous lines). As stated earlier, the other scission-point models overestimate the angular anisotropy by a huge margin. The improvement made by the inclusion of the twisting and wriggling energies in calculating the level density can be appreciated by comparing the long dashed and continuous lines.

The inclusion of the effects arising from the excitation of wriggling and twisting modes is responsible for the improved angular distribution prediction by the present model. The final fragment spins originate from the coupling of these modes and the tilting mode; therefore, a high degree of correlation between the angular distribution and final fragment spin distribution is expected. The good agreement observed between the present model calculation and the experimentally estimated average total fragment spin (table 1, [3]) indicates this correlation. The angular variation of M_γ is another experimental observation which the theoretical models must address. Conspicuous features of the observed angular variation are that the change in M_γ as a function of the angle is small and essentially identical for most systems (§3.3). Some clues on this observation, developed in the premises of the present model, are discussed in [3] and further work on this front is necessary to explain the relevant data.

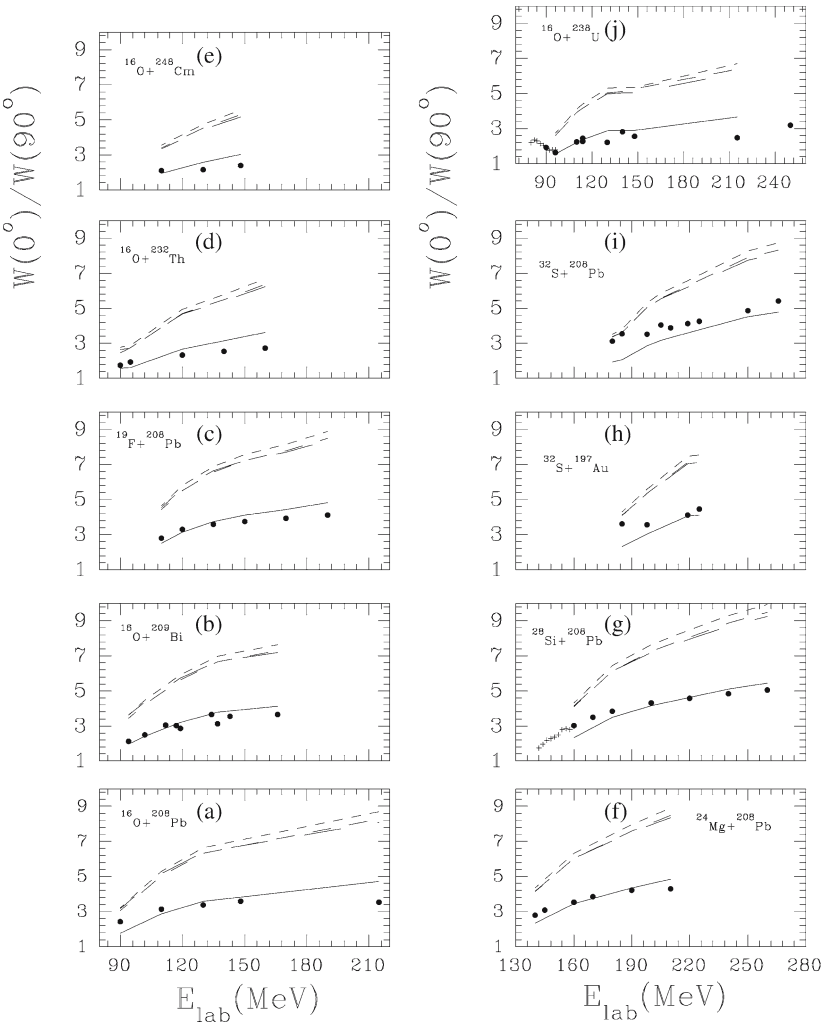

Figure 7. (a)–(j) Angular anisotropy vs. bombarding energy for heavy-ion-induced fission reactions. (•) The experimental data from [22] and (+) data from [35,36]. The lines show the results of various model calculations. The continuous lines indicate the results obtained using the statistical pre-scission-point model [3]. The short-dashed, dashed, and long dashed lines indicate the results obtained using the expressions from [18–20], respectively, as explained in [3].

5. Concluding remarks

A combined statistical dynamical approach to describe fission has emerged in recent years which formulates the transfer of energy between collective and internal degrees of freedom. Due to this transfer, the fast intrinsic degrees of freedom can exert forces on the slow collective degrees of freedom. In the final phases of fission process, there are

fast collective rotational degrees of freedom operational, which can likewise exert forces on the slow collective rotational degrees of freedom. A complete description of the fission process thus depends on the statistical and dynamical nature of the collective rotational degrees of freedom. The emphasis in this article is restricted to the angular momentum-bearing collective degrees of freedom and a statistical description of the same for fission fragment angular and spin distributions.

In short, the experimental approaches that probe the equilibration of rotational degrees of freedom in fission have been briefly discussed. The experimental observations that do not reconcile with either the saddle-point or the scission-point versions of the statistical transition state theory have been emphasized. A new version of the theory, the statistical pre-scission-point model for the fragment angular and spin distributions, in which the transition state is assumed to be the pre-scission point, has been described. The conditional equilibrium of the collective angular momentum-bearing modes at the pre-scission point which is guided mainly by their relaxation times and population probabilities has been taken into account in this model. Dynamical nature of the rotational modes and their influences on the level density of the pre-scission nucleus have been discussed. For this, recourse was taken from the dynamical models, and therefore it may be stated that the present model reconciles with the dynamical aspects. The model predictions have been compared satisfactorily with the experimental data on angular anisotropy and fragment spin for a wide variety of heavy- and light-ion-induced fission reactions.

Acknowledgements

Author gratefully acknowledges D C Biswas for his advice and keen interest during the course of this work.

References

[1] J Randrup and P Moller, *Phys. Scr. T* **150**, 014033 (2012)
[2] G D Adeev, A V Karpov, P N Nadtochy and D V Vanin, *Phys. Part. Nuclei* **36**, 378 (2005) P N Nadtochy, C Schmitt and K Mazurek, *Phys. Scr. T* **154**, 014004 (2013)
[3] Bency John and S K Kataria, *Phys. Rev. C* **57**, 1337 (1998)
[4] I Stetcu, P Talou, T Kawano and M Jandel, *Phys. Rev. C* **90**, 024617 (2014) and references therein
[5] F Gonnenwein, I Tseckhanovich and V Rubchenya, *Int. J. Mod. Phys. E* **16**, 410 (2007)
[6] M Zielinska-Pfabe and K Dietrich, *Phys. Lett. B* **49**, 123 (1974)
[7] I N Mikhailov and P Quentin, *Phys. Lett. B* **462**, 7 (1999)
[8] E Uegaki, *Phys.: Conf. Ser.* **436**, 012049 (2013)
[9] J Randrup, *Nucl. Phys. A* **447**, 133c (1985)
[10] T Dossing and J Randrup, *Nucl. Phys. A* **433**, 215 (1985)
[11] T Dossing and J Randrup, *Phys. Lett. B* **155**, 333 (1985)
[12] R Ramanna, *Phys. Lett.* **10**, 321 (1964)
[13] V S Ramamurthy and R Ramanna, *Pramana – J. Phys.* **33**, 133 (1989) and references therein
[14] L G Moretto, G F Peaslee and G J Woznaik, *Nucl. Phys. A* **502**, 453c (1989)
[15] L G Moretto and G J Woznaik, *Ann. Rev. Nucl. Part. Sci.* **34**, 189 (1984)
[16] J R Nix and W J Swiatecki, *Nucl. Phys.* **71**, 1 (1965)
[17] R Vandendosch and J R Huizenga, *Nuclear fission* (Academic, New York, 1973)
[18] P D Bond, *Phys. Rev. C* **32**, 471 (1985)

[19] H Rossner, J R Huizenga and W U Schroder, *Phys. Rev. C* **33**, 560 (1986)
[20] R Freifelder and M Prakash, *Phys. Rep.* **133**, 315 (1986)
[21] R F Reising, G L Bate and J R Huizenga, *Phys. Rev.* **141**, 1161 (1966)
[22] B B Back, R R Betts, J E Gindler, B D Wilkins, S Saini, M B Tsang, C K Gelbke, W G Lynch, M A McMahan and P A Baisden, *Phys. Rev. C* **32**, 195 (1985)
[23] P N Nadtochy, E G Ryabov, A E Gegechkori, A Yu Anischenko and G D Adeev, *Phys. Rev. C* **89**, 014616 (2014)
[24] T Datta, S P Dange, H Naik and S B Manohar, *Phys. Rev. C* **48**, 221 (1993)
[25] A Goswami, S B Manohar, S K Das, A V R Reddy, B S Tomar and Satya Prakash, *Z. Phys. A* **342**, 299 (1992)
[26] Bency John, A Nijasure, S K Kataria, A Goswami, B S Tomar, A V R Reddy and S B Manohar, *Phys. Rev. C* **51**, 165 (1995)
[27] R P Schmitt, L Cooke, H Dejbakhsh, D R Haenni, T Shutt, B K Srivastava and H Utsunomiya, *Nucl. Phys. A* **592**, 130 (1995)
[28] M Ogihara *et al*, *Z. Phys. A* **335**, 203 (1990)
[29] T Ericson, *Adv. Phys.* **9**, 425 (1960)
[30] A Ya Rusanov, G D Adeev, M G Itkis, A V Karpov, P N Nadtochy, V V Pashkevich, I V Pokrovsky, V S Salamatin and G G Chubarian, *Phys. At. Nucl.* **70**, 1679 (2007)
[31] D J Hinde *et al*, *Phys. Rev. C* **60**, 054602 (1999)
[32] E Vulgaris, L Grodzins, S G Steadman and R Ledoux, *Phys. Rev. C* **33**, 2017 (1986)
[33] W Younes and D Gogny, *Phys. Rev. Lett.* **107**, 132501 (2011)
[34] U Brosa, S Grossmann and A Muller, *Phys. Rep.* **197**, 167 (1990)
[35] D J Hinde, M Dasgupta, J R Leigh, J P Lestone, J C Mein, C R Morton, J O Newton and H Timmers, *Phys. Rev. Lett.* **74**, 1295 (1995)
[36] D J Hinde, C R Morton, M Dasgupta, J R Leigh, J C Mein and H Timmers, *Nucl. Phys. A* **592**, 271 (1995)